General correlation function series: Phase diagram of the anisotropic Heisenberg antiferromagnet in a field

O. G. Mouritsen, E. Kjaersgaard Hansen, and S. J. Knak Jensen
Department of Physical Chemistry, Chemical Institute, Aarhus University, DK-8000 Aarhus C, Denmark
(Received 9 January 1980)

A general scheme is presented to calculate high-temperature series coefficients for ensemble averages of spin operators for spin systems with Hamiltonians containing a large number of model parameters. The scheme, which is based on the moment method, provides the series coefficients as exact functions of the model parameters, e.g., spatial dimensionality, coupling distributions in coordinate and spin space, site-dependent field distributions, and spin quantum number. General expressions for the series coefficients for the auto- and pair-correlation functions are given to sixth order in the case of a classical Hamiltonian with bilinear interactions and a one-component site-dependent magnetic field. The general expressions are used to calculate susceptibility series for the simple cubic anisotropic classical Heisenberg antiferromagnet in a uniform nonordering magnetic field along the easy axis. The series coefficients are polynomials in three variables representing the field, the anisotropy, and the ratio of nearest- and next-nearest-neighbor couplings, respectively. From an analysis of the ordering susceptibility series the phase diagram spanned by the temperature and the field has been calculated for various values of the anisotropy parameter. The calculated phase diagram, which includes a spin-flop phase, an antiferromagnetic phase, and a paramagnetic phase, is in agreement with predictions based on Monte Carlo and renormalization-group calculations.

I. INTRODUCTION

For almost two decades, analysis of series expansions has provided some of the most significant and reliable information on the critical properties of nontrivial lattice models.[1] This information has been of seminal importance in proposing, testing, and corroborating the basic ideas of the scaling and universality hypotheses. Results from series analysis are often considered to be the ultimate judge in assessing predictions of approximate theories for critical phenomena, e.g., the renormalization-group theory.

Series expansion techniques are usually characterized by their specificity to the model and lattice under consideration.[1] Highly specialized techniques are required to obtain the large number of expansion coefficients, which is necessary to determine the finer details of critical behavior. Therefore, only fairly simple models with a few model parameters have been subjected to series analysis.

The purpose of this article is to describe a scheme to calculate high-temperature series for general spin Hamiltonians.[2] The Hamiltonians contain a large number of model parameters describing the coupling distributions in spin and coordinate space. Moreover, we also include symmetry-breaking fields in order to study complete phase diagrams and multicritical phenomena. This implies that the specific and highly optimized methods devised for simple Ising, XY, and Heisenberg models[1] would not be appropriate for our purpose. We require a more general approach allowing for the treatment of many classes of Hamiltonians by the same method, each class being characterized solely by the topology of the interactions. Our approach is based on the well-known moment method.[3] Throughout, the calculation of the series coefficients is carried out utilizing a computer. The basic series obtained by the method are correlation function series from which series for various other quantities can readily be derived. For each class of Hamiltonians the series coefficients are given as exact functions of the model parameters. Thus, a major advantage of our approach is that series for many different models can be derived from the same general expression. The drawback of the general approach is that fewer coefficients can be obtained in the expansions than if more specific methods were applied. This in turn implies that the information on the critical properties extracted from the series is less accurate. Our general series extend to *sixth order* in the inverse temperature. We shall show that valuable information on phase diagrams for complicated antiferromagnetic systems subjected to symmetry-breaking fields may be obtained from these sixth-order series.

Only a few quantitatively reliable calculations of antiferromagnetic phase diagrams have been reported. In most cases the mean-field description is the only one available. One of the reasons for this is that

it is extremely complicated to calculate series for models with more than a few parameters. A small number of papers have been published on series analysis of phase diagrams of Ising antiferromagnets in fields,[4–8] and there appears to be no account published on phase diagrams of Heisenberg-like antiferromagnets. Previous applications of our method to Heisenberg-like antiferromagnetic models are reported in Refs. 2, 9, and 10.

In view of the strong current interest in multicritical points and crossover phenomena[11–22] we have in this paper used our general series to calculate the phase diagram of the three-dimensional anisotropic Heisenberg antiferromagnet in a field. To locate the phase boundaries we have analyzed the ordering susceptibility which is strongly divergent at the boundaries separating the ordered phases (i.e., the spin-flop and the antiferromagnetic phases) and the paramagnetic phase. The susceptibility series are analyzed in terms of a simple power-law singularity using ratio, Neville, and Padé analyses.

The outline of the paper is as follows: In Sec. II we present our scheme for calculating series coefficients with emphasis on the general features, the applicability, and the limitations of the approach. Section III describes the general expressions for the series coefficients to sixth order in the inverse temperature for the auto- and pair-correlation functions in case of a classical Hamiltonian with bilinear interactions and a one-component site-dependent magnetic field. These general expressions are exploited in Sec. IV to calculate the ordering susceptibility series of the simple cubic (sc) anisotropic classical Heisenberg antiferromagnet in a nonordering magnetic field. From an analysis of the ordering susceptibility series the phase diagram spanned by the temperature and the field is calculated as a function of the anisotropy. This section also includes a description of the various checking procedures performed to test our general series. Our results are discussed in Sec. V.

II. CALCULATION OF SERIES COEFFICIENTS

A. Principles of the calculation

We consider a system of N equivalent spins with spin quantum number S. In thermal equilibrium the system is described by the density operator

$$\rho(T)=\exp(-H/k_BT)/\mathrm{Tr}[\exp(-H/k_BT)] \ , \tag{2.1}$$

where H is the Hamiltonian and T is the spin temperature. Following the basic ideas of the moment method,[3] we can expand the ensemble average of a spin operator F in a high-temperature series as

$$\begin{aligned}\langle F\rangle &\equiv \mathrm{Tr}[\rho(K)F] \\ &= \sum_{n=0}^{\infty}\frac{1}{n!}\left[\frac{\partial^n\langle F\rangle}{\partial K^n}\right]_{K=0}K^n \\ &= \sum_{n=0}^{\infty}\frac{(-1)^n}{n!}c_nK^n \ .\end{aligned} \tag{2.2}$$

In Eq. (2.2) we have used the high-temperature expansion variable $K\equiv J/k_BT$, where J is an energy parameter. The coefficients c_n are the cumulants given by

$$\begin{aligned}c_0&=\langle\langle F\rangle\rangle \ , \\ c_1&=\langle\langle FH\rangle\rangle-\langle\langle F\rangle\rangle\langle\langle H\rangle\rangle \ , \\ c_2&=\langle\langle FH^2\rangle\rangle-2\langle\langle FH\rangle\rangle\langle\langle H\rangle\rangle \\ &\quad-\langle\langle F\rangle\rangle\langle\langle H^2\rangle\rangle+2\langle\langle F\rangle\rangle\langle\langle H\rangle\rangle^2 \ , \\ &\vdots\end{aligned} \tag{2.3}$$

with the following definition of the reduced trace

$$\langle\langle\cdots\rangle\rangle=\mathrm{Tr}(\cdots)/(2S+1)^N \ . \tag{2.4}$$

Only Hamiltonians with a finite range of interaction are considered. If we ignore boundary effects we can argue on physical grounds that each coefficient in Eq. (2.2) is of the same order in N as $\langle F\rangle$. For an ensemble average proportional to N, the only part of the cumulant c_n, which contains terms of order N, is $\langle\langle FH^n\rangle\rangle$. In addition, $\langle\langle FH^n\rangle\rangle$ may also contain terms of higher order in N which, however, cancel with the part left of the cumulant. Accordingly, the essential problem in calculating high-temperature series coefficients according to Eqs. (2.2)–(2.4) is to calculate quantities of the form $\mathrm{Tr}(FH^n)$.

We shall consider rather general Hamiltonians, as for example

$$\begin{aligned}H=\sum_{j,u}^{N}&(J_{ju}^{(x)}S_{jx}S_{ux}+J_{ju}^{(y)}S_{jy}S_{uy} \\ &+J_{ju}^{(z)}S_{jz}S_{uz})+\sum_{j}^{N}H_j^{(x)}S_{jx} \ ,\end{aligned} \tag{2.5}$$

where $H_j^{(x)}$ is the x component of a site-dependent magnetic field, and $J_{ju}^{(x)}$, $J_{ju}^{(y)}$, and $J_{ju}^{(z)}$ are coupling constants. For notational simplicity in the description of our computational scheme it is useful to rewrite the Hamiltonian in a compact form as

$$H=\sum_{j=1}^{N}\sum_{i=1}^{M=4}\sum_{u=1}^{L(i)}\prod_{k=1}^{l_i}S_{s_k}^{(i)}B_{mn}^{(i)} \ . \tag{2.6}$$

In Eq. (2.6) the sum over i represents the various types of interactions—or topologies—in which the jth spin is engaged. The ith topology is characterized by

l_i index names, $\{s_1, \ldots, s_{l_i}\}$, denoting the spins involved in the topology. The set $\{s_1, \ldots, s_{l_i}\}$ includes j itself. $L(i)$ is the number of realizations of the ith topology, where a realization gives the actual values of the index names. $B_{nm}^{(i)}$ is a generalized coupling constant, and $m,n \in \{s_1, \ldots, s_{l_i}\}$. In the case of the Hamiltonian in Eq. (2.5) we have $B_{mn}^{(1)} = J_{mn}^{(x)}$, $B_{mn}^{(2)} = J_{mn}^{(y)}$, $B_{mn}^{(3)} = J_{mn}^{(z)}$, and $B_{mm}^{(4)} = H_m^{(x)}$. $S_{s_k}^{(i)}$ denotes one of the components of the spin operator $\vec{S}_{s_k}$.

Actually, our scheme is not restricted to pair interactions, but multispin interactions as well as interactions involving powers of spin operators are also covered by the scheme. Such interactions may be included in our formalism if Eq. (2.6) is generalized to

$$H = \sum_{j=1}^{N} \sum_{i=1}^{M} \sum_{u=1}^{L(i)} \prod_{k=1}^{l_i} O_{s_k}^{(q)} \prod_{m,n \in \{s_1, s_2, \ldots, s_{l_i}\}} B_{mn}^{(t)} , \tag{2.7}$$

where $O_{s_k}^{(q)}$ is a spin operator of type $q = q(k,i)$ belonging to the s_kth spin. $O_{s_k}^{(q)}$ may in the general case be a product of powers of the components of the spin angular momentum operator $\vec{S}_{s_k}$. $B_{mn}^{(t)}$ is a coupling constant of type $t = t(m,n,i)$ associated with the ith topology.

A class of Hamiltonians is defined as the subset of H resulting from a specific choice of the interaction topologies. For each class the lattice structure (including spatial dimensionality), the distribution of coupling and field parameters in coordinate and spin space (including range of interaction), and the spin quantum number appear as variables.

We now turn to the calculation of $\mathrm{Tr}(FH^n)$, where F is a spin operator of type $O^{(q)}$ which may contain fixed indices (e.g., in case of two-point correlation functions). A general term of the trace may be written as

$$\mathrm{Tr}\left(\sum_{k_1,k_2,\ldots,k_n} B_{i_1 j_1}^{(1)} B_{i_2 j_2}^{(2)} \cdots B_{i_l j_l}^{(l)} O_{k_1}^{(1)} O_{k_2}^{(2)} \cdots O_{k_m}^{(m)} \right)$$

$$= \sum_{k_1,\ldots,k_n} B_{i_1 j_1}^{(1)} B_{i_2 j_2}^{(2)} \cdots B_{i_l j_l}^{(l)} \mathrm{Tr}\left(O_{k_1}^{(1)} O_{k_2}^{(2)} \cdots O_{k_m}^{(m)} \right) , \tag{2.8}$$

with the restriction

$$\{i_1, j_1, i_2, j_2, \ldots, i_l, j_l\} \subseteq \{k_1, k_2, \ldots, k_m\} . \tag{2.9}$$

The set $\{k_{n+1}, k_{n+2}, \ldots, k_m\}$ constitutes the fixed indices. The inclusion sign in Eq. (2.9) indicates that each index *name* must appear at a spin operator. Specifying the class of Hamiltonians under consideration is equivalent to giving the actual correspondence between the two sets of index names in Eq. (2.9).

Each term in Eq. (2.8) may be mapped on a linear graph.[23] The indices (or the traces of spin operators $O_j^{(q)}$) correspond to the vertices and the coupling parameters, $B_{ij}^{(t)}$, to the lines (bonds). The calculation procedure of Eq. (2.8) may conveniently be divided into three basic steps: (i) determination of all distinct graphs and their multiplicities; (ii) determination of connected graphs; (iii) embedding of connected graphs in a lattice. We should like to emphasize that steps (i) and (ii) in this approach are fairly general and may be adapted to various homogeneous many-body systems (solid, liquid, or gas) with different degrees of freedom. The connection to the classical Mayer cluster-integral formalism is investigated in detail by Domb.[23]

The series coefficients resulting from steps (i) and (ii) contain a significant amount of configurational information of a general character and it is important to realize that up to this point the result only depends on the interaction topologies chosen. In step (iii) we introduce the spatial configuration of the system (i.e., lattice structure and dimension). This step may also be termed calculation of "lattice constants."[24,25] In the approach of Domb and collaborators all three steps are performed simultaneously in order to reduce the number of contributing graphs taking into account the specific nature of the Hamiltonian and the lattice under consideration. In our case we would gain no advantage by incorporating the embedding procedure in step (i) because practically all distinct connected graphs resulting from steps (i) and (ii) can be embedded in the lattice due to the large number of interacting neighbors in the Hamiltonian.

Nevertheless, we shall impose some restrictions on step (i) of which the symmetry of the Hamiltonian and the properties of the spin-angular-momentum operators make the most significant reduction of the number of contributing graphs. We now proceed to describe in detail our accomplishment of steps (i)–(iii).

B. Step (i) determination of all distinct graphs and their multiplicities

The starting point is Eqs. (2.8) and (2.9), which implies an N^n-fold summation. Even for a simple interaction topology and to a low order this is a tremendous and tedious task. Fortunately, only a limited number of terms are nonzero and only a small number of distinct graphs contribute. In the case of a simple Hamiltonian (e.g., the spin-$\frac{1}{2}$ Ising model in zero field) the few distinct graphs and their multiplicities may be determined by hand to a high order but for the more complex cases which we consider this is not manageable beyond second or third order. We therefore utilize a computer to take care of the necessary "bookkeeping." All operations done by the com-

puter in these calculations are of a symbolic character and the results are *exact* analytical expressions in the chosen variables which have an integer representation in the computer. For convenience, the numerical constants are treated with floating-point arithmetic at the end of the calculation. The calculation procedure to be described below is a generalization of the procedure introduced in the analytical calculation of the higher moments of the magnetic resonance lines of a dipolar coupled rigid lattice.[26]

The sum in Eq. (2.8) is an unrestricted sum, i.e., all summation indices take on all possible values independently. In order to calculate the traces we transform this unrestricted sum into a sum of restricted sums $\sum'$:

$$\sum'_{k_1,k_2,\ldots,k_n} \equiv \sum_{k_1} \sum_{k_2(\neq k_1)} \cdots \sum_{k_n(\neq k_1,k_2,\ldots,k_{n-1})} . \tag{2.10}$$

The sums $\sum'$ are restricted in the sense that no pair of summation indices take on the same value simultaneously. Rewriting the right-hand side of Eq. (2.8) as

$$\sum_{k_1,k_2,\ldots,k_n} P(k_1,k_2,\ldots,k_m) = \sum_{k_1,k_2,\ldots,k_n} E(i_1,j_1,\ldots,i_l,j_l)\,\mathrm{Tr}\left(\prod_{i=1}^{m} O_{k_i}^{(i)}\right) , \tag{2.11}$$

with the restriction Eq. (2.9), the transformation is given by

$$\sum_{k_1,k_2,\ldots,k_n} P(k_1,k_2,\ldots,k_m) = \sum_G \sum'_{i_1,i_2,\ldots,i_{u_G}} P^G(i_1,i_2,\ldots,i_{u_G}) . \tag{2.12}$$

In the Gth restricted sum in Eq. (2.12) the indices $k_1,k_2,\ldots,k_m$ are divided into u_G groups and all indices in a group are substituted by a single new index. $P^G(i_1,i_2,\ldots,i_{u_G})$ is obtained by making this substitution in $P(k_1,k_2,\ldots,k_m)$. In other words, $\sum_G$ is a sum of all groupings of summation indices, each grouping being a disjunctive coverage of the set $\{k_1,k_2,\ldots,k_m\}$. If fixed indices are contained in the set, as in the case of F being a two-point correlation function, their names are kept fixed in order to identify these at the end of the calculation. Using the transformation, Eq. (2.12), in Eq. (2.11) we obtain

$$\sum_{k_1,k_2,\ldots,k_n} E(i_1,j_1,\ldots,i_l,j_l)\,\mathrm{Tr}\left(\prod_{i=1}^{m} O_{k_i}^{(i)}\right) = \sum_G \sum'_{i_1,i_2,\ldots,i_{u_G}} E^G(i_1,i_2,\ldots,i_{u_G})\,\mathrm{Tr}\left(\prod_{p=1}^{u_G} O_{i_p}^{(G,p)}\right)$$
$$= \sum_G (2S+1)^{N-u_G} \left(\prod_{p=1}^{u_G} \mathrm{tr}\,(O^{(G,p)})\right)\left(\sum'_{i_1,i_2,\ldots,i_{u_G}} E^G(i_1,i_2,\ldots,i_{u_G})\right) . \tag{2.13}$$

All spin operators with index i_p are collected in the operator $O^{(G,p)}$. The trace $\mathrm{tr}(O^{(G,p)})$ is defined on the space of a single spin variable. Equation (2.13) is the basic equation of step (i).

In evaluating Eq. (2.13) we use the property of the spin angular momentum operators that $\mathrm{tr}[(S_x)^{n_x}(S_y)^{n_y}(S_z)^{n_z}]$ is zero unless n_x, n_y, and n_z are all even or all odd integers.[27]

An alternative formulation of the calculation contained in step (i) may be given in the context of graph theory. It is very instructive to make a graph representation of the arithmetic process Eqs. (2.8) through (2.13) but we emphasize that our approach is purely algebraic and makes no use of graph-theoretical theorems or simplifications introduced by a graph representation. This is strongly coupled with the basic problem of the distinction between labeled and unlabeled graphs.[23] Using a computer we necessarily have to work with labeled graphs. The procedure in going from Eq. (2.8) to Eq. (2.13) corresponds in graph theoretical language to the determination of all distinct graphs (and their multiplicities) which can be constructed from the m vertices, $\{k_1,k_2,\ldots,k_m\}$, and the l lines

$$\{B_{i_1j_1}^{(1)}, B_{i_2j_2}^{(2)}, \ldots, B_{i_lj_l}^{(l)}\} .$$

Both the lines and the vertices may overlap in the resulting graphs which can be either connected or disconnected.[23] Each vertex corresponds to a trace of spin operators. In the construction of the different traces the noncommutativity of the spin operators must be taken into account. The computer program

determines *all* graphs and sums up the number of identical graphs in order to determine their multiplicities. This implies that the calculation of the multiplicities by our method consumes the major part of the computation time in contrast to other current methods[23,28] which often determine these numbers by a simple combinatorial formula.

The final result of step (i) is a sum of terms each characterized by a graph and a linear combination of single spin traces. The values of the necessary traces are given in Ref. 27 or may easily be evaluated algebraically on a computer.[26] All quantum mechanical traces are polynomials in $S(S+1)$.

In this work we restrict ourselves to classical spins, i.e., the limit $S \to \infty$, $\hbar \to 0$, $\hbar S$ finite. The traces then reduce to integrals over the solid angle of each unit spin vector. The classical limit causes a considerable reduction in the number of different terms resulting from step (i).

C. Step (ii) determination of connected graphs

The graphs resulting from step (i) are either connected or disconnected. Each graph, which corresponds to a restricted sum, is termed a restricted graph. Due to the property of the cumulants in Eq. (2.3) we have to consider only connected graphs. If the property under consideration is of order N^p a disconnected restricted graph contains terms of the order N^p and N^{p+1}, N^{p+2}, . . . , N^{p+n}, where $n+1$ is the number of disconnected constituents (subgraphs) of the graph. This entails that the disconnected graphs—in their capacity of being restricted—contain a connected part which must be isolated.

Step (ii) aims at isolating all connected graphs from step (i) and to determine the lowest order contribution from each disconnected graph. This simple procedure is illustrated by the example

$$\begin{aligned}
&\sum_{k,l,m,i,j}{}' B_{kl}B_{lm}B_{mk}B_{ij}A_{jj} \\
&= \left(\sum_{k,l,m}{}' B_{kl}B_{lm}B_{mk}\right)\left(\sum_{i,j}{}' B_{ij}A_{jj}\right) \\
&\quad - 3\sum_{k,l,m,j}{}' B_{kl}B_{lm}B_{mk}B_{kj}A_{jj} - 3\sum_{k,l,m,j}{}' B_{kl}B_{lm}B_{mk}B_{kj}A_{kk} \\
&\quad - 6\sum_{k,l,m}{}' B_{kl}B_{lm}(B_{mk})^2A_{kk} \quad , \qquad (2.14)
\end{aligned}$$

where B_{mn} may denote a two-site coupling constant and A_{mm} a one-site coupling constant, e.g., a field. Step (ii) is also programmed for a computer and the output contains connected restricted graphs only.

D. Step (iii) embedding of connected graphs in a lattice

This final step assumes a specific underlying lattice in which the graphs are to be embedded or, alternatively, the lattice constants are to be evaluated. The distribution of coupling parameters, B, now has to be specified including the number of interacting neighbors and the range of interaction. In the case of a large number of interacting neighbors with different strength of interaction the embedding problem is almost as time consuming as the determination of the multiplicities of the graphs in step (i). The calculation may in some cases be substantially reduced by taking into account the spatial symmetry of the distribution B. In the case of calculating properties with site-dependent weight factors (e.g., the staggering index for the ordering susceptibility of antiferromagnets) only the common symmetry of the distribution B and the weight factors can be exploited.

Step (iii) is also programmed for a computer. We refer to Ref. 29 for a detailed description of computer techniques for evaluating lattice constants. In our case the calculation is straightforward: fix one vertex at some site of the lattice and vary the rest of the vertices on the lattice sites with the restrictions imposed through B. Due to the fact that we deal exclusively with restricted sums (or graphs) the calculation of the embeddings is closely related to the excluded volume problem.[30] In Sec. IV C we describe the checking of the computer program.

III. CORRELATION FUNCTION SERIES

In this section we use our scheme to calculate the high-temperature series for the auto- and pair-correlation functions in the case of a bilinear spin Hamiltonian with a site-dependent magnetic field

$$\begin{aligned}
H = \sum_{j=1}^{N}\sum_{l=1(\neq j)}^{N} &[A(j,l)S_{jx}S_{lx} + B(j,l)S_{jy}S_{ly} \\
&+ C(j,l)S_{jz}S_{lz}] + \sum_{j=1}^{N} H(j)S_{jz} \quad . \qquad (3.1)
\end{aligned}$$

The Hamiltonian is classical, $S=\infty$, and the spin at each of the N lattice points is represented by a unit vector $\vec{S}_j = (S_{jx}, S_{jy}, S_{jz})$. $A(j,l)$, $B(j,l)$, and $C(j,l)$ represent pair coupling distributions, and $H(j)$ denotes a site-dependent magnetic field.

The Hamiltonian in Eq. (3.1) includes well-known classical models, such as the Ising, the XY, and the Heisenberg models defined on lattices of arbitrary structure and dimension. Furthermore, arbitrary ranges of interaction and degrees of anisotropy in spin and coordinate space may be considered. The inclusion of the field term in Eq. (3.1) makes it possible to use the series in investigations of phase di-

agrams spanned by two thermodynamic variables, the temperature and a field parameter.

The auto- and pair-spin-correlation functions are defined by

$$\Gamma_{\alpha\beta}(\vec{r}_{jl},T)=\delta_{\alpha\beta}\langle S_{j\alpha}S_{l\alpha}\rangle/\mathrm{Tr}(S_{j\alpha}^2)\ ,\quad \alpha,\beta=x,z\ , \tag{3.2}$$

with $\vec{r}_{jl}=\vec{0}$ and $\vec{r}_{jl}\neq\vec{0}$, respectively. The classical property of H implies that any susceptibility is related to the fluctuations in the corresponding magnetization through the fluctuation theorem.[31] For a system with an antiferromagnetic ordered state we therefore obtain components of the bulk and staggered susceptibilities as

$$\chi^b_{\alpha\alpha}(T)=(k_BT)^{-1}\sum_{j,l}\Gamma_{\alpha\alpha}(\vec{r}_{jl},T)\ , \tag{3.3}$$

and

$$\chi^s_{\alpha\alpha}(T)=(k_BT)^{-1}\sum_{j,l}e^{i\vec{k}\cdot\vec{r}_{jl}}\Gamma_{\alpha\alpha}(\vec{r}_{jl},T)\ , \tag{3.4}$$

respectively. $\vec{k}$ is the propagation vector defining the magnetic structure below the transition. As the ordering susceptibility we use $\chi^s_{\alpha'\alpha'}(T)$ with α' denoting the ordering component of the spin vectors.

The high-temperature series expansion of $\Gamma_{\alpha\alpha}(\vec{r}_{jl},T)$ may be written

$$\Gamma_{\alpha\alpha}(\vec{r}_{jl},T)=\sum_{k=0}^{\infty}q_k^{\alpha\alpha}(\vec{r}_{jl},A,B,C,H)K^k\ , \tag{3.5}$$

$$\alpha=x,z,\quad K=J/k_BT\ .$$

The expansion coefficients $q_k^{\alpha\alpha}$ are functions of restricted lattice sums (cf. Sec. II) involving the coupling distributions $A(j,l)$, $B(j,l)$, $C(j,l)$, and $H(j)$, which constitute the model parameters. Some of the graphs contributing to $\Gamma_{zz}(\vec{r}_{jl},T)$, $\vec{r}_{jl}\neq\vec{0}$, are disconnected due to the long-ranged field-induced pair correlation. When the correlation functions are used in susceptibility calculations through Eqs. (3.3) and (3.4) the disconnected contributions vanish.

The coefficients q_k^{xx} and q_k^{zz} for the auto- and pair-correlation functions are given to sixth order in K in Ref. 32.

IV. ANISOTROPIC HEISENBERG ANTIFERROMAGNET IN A FIELD

A. Field-dependent critical behavior

In the study of field-dependent critical phenomena it is important to distinguish between ordering and nonordering fields.[33] A finite ordering field will destroy the transition, whereas it may be preserved in a nonordering field, although the nature of the transition and the position of the phase boundaries may be changed. The field, which is a symmetry-breaking parameter, can for example be an external stress or a magnetic field. Variation of fields often leads to complex phase diagrams with multicritical points.

In the past decade there has been an increasing interest in investigating the field dependence of the critical properties of magnetic coupled systems. The reader is referred to the comprehensive review by de Jongh and Miedema[18] and to Refs. 19–22 for descriptions of experimental investigations of systems in magnetic fields.

In this section we perform a high-temperature series study of an antiferromagnetic model subjected to a symmetry-breaking magnetic field. The model includes spin-space anisotropy and is therefore expected to exhibit various kinds of critical behavior. The model is a Heisenberg Hamiltonian with uniaxial anisotropy defined by

$$H=J_1\sum_{j,l(\neq j)}^{\mathrm{nn}}[(1-\Delta)(S_{jx}S_{lx}+S_{jy}S_{ly})+S_{jz}S_{lz}]+J_2\sum_{j,l(\neq j)}^{\mathrm{nnn}}[(1-\Delta)(S_{jx}S_{lx}+S_{jy}S_{ly})+S_{jz}S_{lz}]$$
$$+\mu H_{\parallel}\sum_j S_{jz}+\mu H_{\perp}\sum_j S_{jx}+\mu H_{\parallel}^{+}\sum_j e^{i\vec{k}\cdot\vec{r}_j}S_{jz}\ . \tag{4.1}$$

The model is classical, $S=\infty$, and defined on a sc lattice. J_1 and J_2 are the nearest and next-nearest neighbor exchange-coupling constants taken to be positive and negative, respectively, in order to stabilize the magnetic ground state. μ is the magnetic moment. Δ is the uniaxial anisotropy parameter. We shall restrict ourselves to the case of prolate anisotropy, $0\leq\Delta\leq1$, which makes the z direction the easy axis. $H_{\parallel}$, $H_{\perp}$, and $H_{\parallel}^{+}$ are field parameters, and $\vec{k}$ is the propagation vector of the ordered state. It should be noted that the model in Eq. (4.1) reduces to the $S=\infty$ XY model in the limit $\Delta\to\infty$ and to the $S=\infty$ Ising model for $\Delta=1$.

The Heisenberg antiferromagnet with various degrees of anisotropy is a useful model for describing a variety of magnetic materials. Well-known examples[18] described by the model are for $\Delta\neq0$: $CuCl_2\cdot2H_2O$, $GdAlO_3$, $MnCl_2\cdot4H_2O$, FeF_2, MnF_2 and for $\Delta\simeq0$: $RbMnF_3$ and $KNiF_3$.

The model in Eq. (4.1) has been studied in the limit $H_{\parallel}^{+}=0$ by means of mean-field theory.[34–36] A more accurate investigation of the critical behavior of

the model with all fields included has been performed in the framework of renormalization-group theory.[12–14] Recently, Landau and Binder[17] investigated the phase diagram of the model with $J_2=0$ by means of spin-wave and Monte Carlo calculations. Landau and Binder determined the phase diagram quantitatively for $\Delta=0$ and 0.2 and found their results to be in agreement with the renormalization-group predictions. Our work focuses on the $(T,H_{\parallel})$ plane of the phase diagram which is shown qualitatively in Fig. 1. At low temperatures and low fields the ordered state is a simple type-I antiferromagnet, AF, with sublattice magnetizations along the field. The AF phase is separated from the paramagnetic phase by a second-order phase boundary associated with $n=1$ Ising critical behavior, where n denotes the number of components of the order parameter. For a sufficiently large field the system displays the phenomenon of spin flopping associated with first-order transitions from the AF phase to the spin-flop phase (SF). In the spin-flop phase the magnetic moments order in the x and y components of the spin vectors. The angle between the spin vectors and the z direction defines the canting angle which varies from 90° at the spin-flop line to 0° at the phase boundary separating the SF phase and the paramagnetic (P) phase. This boundary consists of second-order transitions belonging to the $n=2\chi XY$ universality class. The three phase boundary lines meet at the *bicritical point* where the two ordered phases become critical simultaneously. At the bicritical point the phase transition is of second order with $n=3$ Heisenberg critical behavior. The crossover between the different kinds of critical behavior at the bicritical point has been investigated in Refs. 11 and 15. The bicritical point may under certain circumstances be turned into a tetracritical point.[16,37,38]

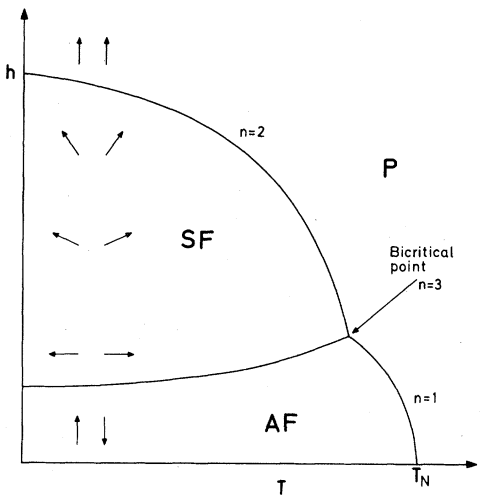

FIG. 1. Qualitative features of the (T,h) plane of the phase diagram for the anisotropic Heisenberg antiferromagnet in a uniform external field, h, along the easy axis. The phase boundary separating the antiferromagnetic phase (AF) and the paramagnetic phase (P) is a line of second-order transitions belonging to the $n=1$ universality class. The phase boundary separating the spin-flop phase (SF) and the paramagnetic phase corresponds to second-order transitions belonging to the $n=2$ universality class. The boundary separating the SF and the AF phase is a line of first-order transitions. The three phase boundaries meet at the bicritical point where the transition is of second-order belonging to the $n=3$ universality class.

B. Susceptibility series

From the general expressions of the correlation functions in Ref. 32 we have calculated components of the bulk and staggered susceptibilities for the Hamiltonian in Eq. (4.1) with $H_{\parallel}^{+}=H_{\perp}=0$, by relating the parameters in Eqs. (3.1) and (4.1). The propagation vector of the antiferromagnetic ordered phase and the spin-flop phase is

$$\vec{k}=\frac{2\pi}{r_0}\left(\tfrac{1}{2},\tfrac{1}{2},\tfrac{1}{2}\right) , \tag{4.2}$$

corresponding to a type-I sc antiferromagnet. r_0 is the sc lattice parameter. For convenience we introduce the reduced susceptibilities

$$\bar{\chi}^{r}_{\alpha\alpha}(T)\equiv N^{-1}\chi^{r}_{\alpha\alpha}(T)k_B T, \quad r=b,s . \tag{4.3}$$

The series for the reduced susceptibilities may now be written

$$\bar{\chi}^{r}_{\alpha\alpha}(K,\tau,\Delta,h)=\sum_{k=0}^{\infty} a^{r}_{\alpha,k}(\tau,\Delta,h)K^{k} , \tag{4.4}$$

$$r=b,s,\ \alpha=x,z ,$$

with $a^{r}_{\alpha,0}=1$ and $K=J/k_B T$. The coefficients $a^{r}_{\alpha,k}$ are functions of the model parameters $\tau\equiv J_2/J_1=J_2/J$, Δ, and $h\equiv\mu H_{\parallel}/J$, and are given by the triple polynomials

$$a^{r}_{\alpha,k}(\tau,\Delta,h)=\sum_{n_\tau,n_\Delta,n_h} W^{r}_{\alpha,k}(n_\tau,n_\Delta,n_h)\tau^{n_\tau}(1-\Delta)^{n_\Delta}h^{n_h} . \tag{4.5}$$

Only even powers of the field are involved due to inversion symmetry in spin space. In a type-I sc antiferromagnetic structure the nearest neighbors and the next-nearest neighbors belong to separate sublattices. This implies the simple relation

$$W^{b}_{\alpha,k}(n_\tau,n_\Delta,n_h=0)=(-1)^{k+n_\tau}W^{s}_{\alpha,k}(n_\tau,n_\Delta,n_h=0) . \tag{4.6}$$

The coefficients $W^{r}_{\alpha,k}(n_\tau,n_\Delta,n_h)$, $0\leq k, n_\tau, n_\Delta, n_h\leq 6$, are given in Tables I and II for the functions $\bar{\chi}^{s}_{xx}$ and $\bar{\chi}^{s}_{zz}$, respectively.

TABLE I. Coefficients $W^{s}_{\chi,k}(n_\tau, n_\Delta, n_h)$ through order $k=6$ in the high-temperature series for the susceptibility in Eqs. (4.4) and (4.5). Only nonzero coefficients are given.

k	n_τ	n_h	$n_\Delta=0$	$n_\Delta=1$	$n_\Delta=2$	$n_\Delta=3$	$n_\Delta=4$	$n_\Delta=5$	$n_\Delta=6$
0	0	0	$0.100\,000\,00\times10^{1}$						
1	0	0		$0.400\,000\,00\times10^{1}$					
1	1	0		$-0.800\,000\,00\times10^{1}$					
2	0	0	$-0.533\,333\,33$		$0.138\,666\,67\times10^{2}$				
2	0	2	$-0.666\,666\,67\times10^{-1}$						
2	1	0			$-0.640\,000\,00\times10^{2}$				
2	2	0	$-0.106\,666\,67\times10^{1}$		$0.597\,333\,33\times10^{2}$				
3	0	0		$-0.412\,444\,44\times10^{1}$		$0.475\,022\,22\times10^{2}$			
3	0	2	$0.533\,333\,33$	$-0.533\,333\,33$					
3	1	0	$0.426\,666\,67\times10^{1}$	$0.853\,333\,33\times10^{1}$		$-0.332\,800\,00\times10^{3}$			
3	1	2	$0.106\,666\,67\times10^{1}$	$0.106\,666\,67\times10^{1}$					
3	2	0		$-0.853\,333\,33\times10^{1}$		$0.733\,866\,67\times10^{3}$			
3	3	0	$0.284\,444\,44\times10^{1}$	$0.167\,822\,22\times10^{2}$		$-0.433\,493\,33\times10^{3}$			
4	0	0	$-0.156\,444\,44\times10^{1}$		$-0.197\,214\,81\times10^{2}$		$0.157\,582\,22\times10^{3}$		
4	0	2	$-0.278\,857\,14\times10^{1}$	$0.412\,444\,44\times10^{1}$	$-0.265\,142\,86\times10^{1}$				
4	0	4	$0.634\,920\,63\times10^{-2}$						
4	1	0		$0.326\,162\,96\times10^{2}$	$0.993\,659\,26\times10^{2}$		$-0.152\,007\,11\times10^{4}$		
4	1	2	$-0.128\,000\,00\times10^{2}$		$0.128\,000\,00\times10^{2}$				
4	2	0	$-0.372\,215\,87\times10^{2}$	$-0.675\,081\,48\times10^{2}$	$-0.133\,390\,90\times10^{3}$		$0.513\,625\,40\times10^{4}$		
4	2	2	$-0.119\,771\,43\times10^{2}$	$-0.167\,822\,22\times10^{2}$	$-0.117\,028\,57\times10^{2}$				
4	3	0		$0.227\,555\,56\times10^{2}$	$0.202\,524\,44\times10^{3}$		$-0.729\,088\,00\times10^{4}$		
4	4	0	$-0.132\,063\,49\times10^{2}$	$-0.439\,940\,74\times10^{2}$	$-0.180\,093\,97\times10^{3}$		$0.309\,264\,25\times10^{4}$		
5	0	0		$-0.107\,198\,79\times10^{2}$		$-0.850\,327\,64\times10^{2}$		$0.520\,297\,26\times10^{3}$	
5	0	2	$0.130\,844\,44\times10^{2}$	$-0.210\,488\,89\times10^{2}$	$0.197\,214\,81\times10^{2}$	$-0.117\,570\,37\times10^{2}$			
5	0	4	$-0.137\,142\,86$	$0.685\,714\,29\times10^{-1}$					
5	1	0	$0.379\,042\,54\times10^{2}$	$0.224\,015\,80\times10^{2}$	$0.150\,157\,77\times10^{3}$	$0.646\,127\,75\times10^{3}$		$-0.630\,376\,57\times10^{4}$	
5	1	2	$0.899\,657\,14\times10^{2}$	$-0.556\,696\,31\times10^{2}$	$-0.584\,601\,06\times10^{2}$	$0.858\,209\,52\times10^{2}$			
5	1	4	$-0.274\,285\,71$	$-0.137\,142\,86$					
5	2	0		$-0.279\,943\,90\times10^{3}$	$-0.781\,172\,94\times10^{3}$	$-0.167\,561\,80\times10^{4}$		$0.294\,992\,91\times10^{5}$	
5	2	2	$0.196\,510\,48\times10^{3}$	$0.107\,276\,19\times10^{3}$	$-0.110\,039\,37\times10^{3}$	$-0.193\,747\,30\times10^{3}$			
5	3	0	$0.292\,614\,77\times10^{3}$	$0.574\,884\,80\times10^{3}$	$0.822\,913\,13\times10^{3}$	$0.219\,304\,32\times10^{4}$		$-0.646\,332\,04\times10^{5}$	
5	3	2	$0.117\,516\,19\times10^{3}$	$0.185\,511\,96\times10^{3}$	$0.180\,093\,97\times10^{3}$	$0.111\,177\,14\times10^{3}$			
5	4	0		$-0.101\,099\,68\times10^{3}$	$-0.533\,997\,04\times10^{3}$	$-0.302\,453\,84\times10^{4}$		$0.667\,569\,98\times10^{5}$	
5	5	0	$0.625\,019\,26\times10^{2}$	$0.194\,179\,71\times10^{3}$	$0.461\,786\,07\times10^{3}$	$0.168\,098\,38\times10^{4}$		$-0.218\,153\,04\times10^{5}$	
6	0	0	$-0.821\,865\,99\times10^{1}$		$-0.437\,188\,75\times10^{2}$		$-0.339\,854\,48\times10^{3}$		$0.169\,329\,54\times10^{4}$
6	0	2	$-0.562\,954\,26\times10^{2}$	$0.971\,019\,80\times10^{2}$	$-0.958\,991\,87\times10^{2}$	$0.850\,327\,64\times10^{2}$	$-0.477\,766\,05\times10^{2}$		
6	0	4	$0.157\,291\,01\times10^{1}$	$-0.132\,740\,74\times10^{1}$	$0.416\,507\,94$				
6	0	6	$-0.634\,920\,63\times10^{-3}$						
6	1	0		$0.268\,278\,20\times10^{3}$	$0.230\,819\,42\times10^{3}$	$0.629\,692\,15\times10^{3}$	$0.350\,712\,41\times10^{4}$		$-0.249\,660\,40\times10^{5}$
6	1	2	$-0.528\,839\,11\times10^{3}$	$0.482\,396\,11\times10^{3}$	$0.386\,266\,53\times10^{2}$	$-0.469\,746\,91\times10^{3}$	$0.477\,563\,26\times10^{3}$		
6	1	4	$0.690\,793\,65\times10^{1}$		$-0.207\,238\,10\times10^{1}$				
6	2	0	$-0.590\,073\,74\times10^{3}$	$-0.556\,709\,25\times10^{3}$	$-0.144\,136\,68\times10^{4}$	$-0.494\,602\,23\times10^{4}$	$-0.132\,331\,81\times10^{5}$		$0.147\,526\,59\times10^{6}$
6	2	2	$-0.175\,146\,26\times10^{4}$	$0.121\,297\,95\times10^{3}$	$0.147\,334\,64\times10^{4}$	$0.174\,372\,57\times10^{3}$	$-0.165\,747\,13\times10^{4}$		
6	2	4	$0.659\,978\,84\times10^{1}$	$0.541\,798\,94\times10^{1}$	$0.186\,920\,63\times10^{1}$				
6	3	0		$0.218\,661\,38\times10^{4}$	$0.655\,157\,73\times10^{4}$	$0.121\,096\,74\times10^{5}$	$0.255\,355\,19\times10^{5}$		$-0.449\,181\,66\times10^{6}$
6	3	2	$-0.246\,715\,73\times10^{4}$	$-0.214\,747\,43\times10^{4}$	$0.789\,509\,42\times10^{2}$	$0.215\,635\,98\times10^{4}$	$0.237\,932\,09\times10^{4}$		
6	4	0	$-0.228\,682\,19\times10^{4}$	$-0.446\,413\,84\times10^{4}$	$-0.635\,362\,77\times10^{4}$	$-0.100\,391\,21\times10^{5}$	$-0.330\,447\,69\times10^{5}$		$0.720\,660\,58\times10^{6}$
6	4	2	$-0.107\,103\,86\times10^{4}$	$-0.179\,938\,08\times10^{4}$	$-0.194\,215\,57\times10^{4}$	$-0.168\,098\,38\times10^{4}$	$-0.977\,688\,57\times10^{3}$		
6	5	0		$0.475\,742\,81\times10^{3}$	$0.225\,543\,57\times10^{4}$	$0.786\,917\,45\times10^{4}$	$0.366\,926\,92\times10^{5}$		$-0.579\,603\,57\times10^{6}$
6	6	0	$-0.316\,749\,77\times10^{3}$	$-0.907\,918\,80\times10^{3}$	$-0.191\,854\,69\times10^{4}$	$-0.423\,602\,15\times10^{4}$	$-0.145\,903\,70\times10^{5}$		$0.152\,664\,03\times10^{6}$

TABLE II. Coefficients $W^s_{z,k}(n_\tau, n_\Delta, n_h)$ through order $k=6$ in the high-temperature series for the susceptibility in Eqs. (4.4) and (4.5). Only nonzero coefficients are given. Note that $W^s_{z,k}(n_\tau, n_\Delta=1, n_h)$ vanishes.

k	n_τ	n_h	$n_\Delta=0$	$n_\Delta=2$	$n_\Delta=3$	$n_\Delta=4$	$n_\Delta=5$	$n_\Delta=6$
0	0	0	$0.100\,000\,00\times10^{1}$					
1	0	0	$0.400\,000\,00\times10^{1}$					
1	1	0	$-0.800\,000\,00\times10^{1}$					
2	0	0	$0.144\,000\,00\times10^{2}$	$-0.106\,666\,67\times10^{1}$				
2	0	2	$-0.200\,000\,00$					
2	1	0	$-0.640\,000\,00\times10^{2}$					
2	2	0	$0.608\,000\,00\times10^{2}$	$-0.213\,333\,33\times10^{1}$				
3	0	0	$0.516\,266\,67\times10^{2}$	$-0.824\,888\,89\times10^{1}$				
3	1	0	$-0.345\,600\,00\times10^{3}$	$0.170\,666\,67\times10^{2}$	$0.853\,333\,33\times10^{1}$			
3	1	2	$0.640\,000\,00\times10^{1}$					
3	2	0	$0.742\,400\,00\times10^{3}$	$-0.170\,666\,67\times10^{2}$				
3	3	0	$-0.453\,120\,00\times10^{3}$	$0.335\,644\,44\times10^{2}$	$0.568\,888\,89\times10^{1}$			
4	0	0	$0.180\,195\,56\times10^{3}$	$-0.420\,977\,78\times10^{2}$		$-0.180\,148\,15\times10^{1}$		
4	0	2	$-0.519\,619\,05\times10^{1}$	$0.538\,412\,70$				
4	0	4	$0.317\,460\,32\times10^{-1}$					
4	1	0	$-0.165\,205\,33\times10^{4}$	$0.198\,731\,85\times10^{3}$	$0.652\,325\,93\times10^{2}$			
4	2	0	$0.537\,990\,10\times10^{4}$	$-0.277\,834\,50\times10^{3}$	$-0.135\,016\,30\times10^{3}$	$-0.689\,168\,25\times10^{2}$		
4	2	2	$-0.123\,032\,38\times10^{3}$	$0.164\,571\,43\times10^{1}$				
4	3	0	$-0.751\,616\,00\times10^{4}$	$0.405\,048\,89\times10^{3}$	$0.455\,111\,11\times10^{2}$			
4	4	0	$0.333\,535\,49\times10^{4}$	$-0.371\,023\,92\times10^{3}$	$-0.879\,881\,48\times10^{2}$	$-0.209\,947\,09\times10^{2}$		
5	0	0	$0.628\,119\,12\times10^{3}$	$-0.194\,203\,96\times10^{3}$		$-0.937\,054\,17\times10^{1}$		
5	0	4	$-0.200\,634\,92$					
5	1	0	$-0.721\,134\,39\times10^{4}$	$0.136\,893\,09\times10^{4}$	$0.325\,613\,94\times10^{3}$	$0.191\,146\,67\times10^{2}$	$0.505\,101\,09\times10^{2}$	
5	1	2	$0.244\,540\,95\times10^{3}$	$-0.240\,558\,73\times10^{2}$	$-0.525\,544\,97\times10^{1}$			
5	1	4	$-0.205\,714\,29\times10^{1}$					
5	2	0	$0.322\,874\,03\times10^{5}$	$-0.345\,398\,99\times10^{4}$	$-0.156\,234\,59\times10^{4}$	$-0.508\,510\,81\times10^{3}$		
5	3	0	$-0.686\,919\,57\times10^{5}$	$0.466\,627\,59\times10^{4}$	$0.171\,623\,12\times10^{4}$	$0.104\,487\,73\times10^{4}$	$0.514\,824\,58\times10^{3}$	
5	3	2	$0.185\,344\,00\times10^{4}$	$-0.650\,158\,73\times10^{2}$	$-0.552\,634\,92\times10^{1}$			
5	4	0	$0.704\,690\,79\times10^{5}$	$-0.615\,396\,91\times10^{4}$	$-0.106\,799\,41\times10^{4}$	$-0.149\,753\,23\times10^{3}$		
5	5	0	$-0.243\,502\,45\times10^{5}$	$0.359\,876\,17\times10^{4}$	$0.957\,756\,05\times10^{3}$	$0.287\,054\,37\times10^{3}$	$0.908\,199\,51\times10^{2}$	
6	0	0	$0.216\,257\,91\times10^{4}$	$-0.826\,481\,78\times10^{3}$		$-0.263\,672\,05\times10^{2}$		$-0.822\,674\,39\times10^{1}$
6	0	2	$-0.951\,029\,36\times10^{2}$	$0.229\,273\,83\times10^{2}$		$0.877\,069\,29$		
6	0	4	$0.269\,714\,29\times10^{1}$	$-0.145\,608\,47$				
6	0	6	$-0.444\,444\,44\times10^{-2}$					
6	1	0	$-0.301\,661\,84\times10^{5}$	$0.792\,106\,34\times10^{4}$	$0.148\,102\,99\times10^{4}$	$0.119\,054\,04\times10^{3}$	$0.314\,910\,74\times10^{3}$	
6	1	4	$0.150\,755\,56\times10^{2}$					
6	2	0	$0.169\,771\,39\times10^{6}$	$-0.284\,546\,28\times10^{5}$	$-0.105\,937\,54\times10^{5}$	$-0.252\,115\,18\times10^{4}$	$-0.643\,108\,12\times10^{3}$	$-0.799\,517\,73\times10^{3}$
6	2	2	$-0.659\,130\,92\times10^{4}$	$0.649\,638\,60\times10^{3}$	$0.219\,522\,48\times10^{3}$	$0.464\,068\,85\times10^{2}$		
6	2	4	$0.699\,428\,57\times10^{2}$	$-0.507\,936\,51$				
6	3	0	$-0.497\,629\,53\times10^{6}$	$0.545\,689\,49\times10^{5}$	$0.248\,503\,96\times10^{5}$	$0.116\,697\,23\times10^{5}$	$0.374\,217\,88\times10^{4}$	
6	4	0	$0.780\,531\,92\times10^{6}$	$-0.712\,500\,24\times10^{5}$	$-0.216\,872\,23\times10^{5}$	$-0.116\,636\,00\times10^{5}$	$-0.764\,385\,50\times10^{4}$	$-0.381\,511\,29\times10^{4}$
6	4	2	$-0.241\,202\,82\times10^{5}$	$0.147\,994\,39\times10^{4}$	$0.205\,103\,41\times10^{3}$	$0.214\,916\,16\times10^{2}$		
6	5	0	$-0.628\,662\,24\times10^{6}$	$0.765\,946\,18\times10^{5}$	$0.160\,603\,65\times10^{5}$	$0.306\,726\,31\times10^{4}$	$0.629\,469\,23\times10^{3}$	
6	6	0	$0.176\,742\,66\times10^{6}$	$-0.325\,198\,17\times10^{5}$	$-0.918\,738\,54\times10^{4}$	$-0.271\,919\,70\times10^{4}$	$-0.120\,344\,17\times10^{4}$	$-0.418\,396\,75\times10^{3}$

C. Checking procedures

The coefficients in Tables I and II as well as those for the bulk susceptibilities may be checked in various limiting cases of the variables by comparison with results for well-known models reported in the literature. The checking provides an integral test of our computer programs used for the accomplishment of steps (i)–(iii) in Sec. II.

Wood and Dalton[39] have calculated the high-temperature series to sixth order for the zero-field susceptibility of the anisotropic nearest-neighbor Heisenberg model. The series coefficients are given as functions of the anisotropy parameter, the lattice structure, and the spin quantum number. In the limit $h=\tau=0$ and $S=\infty$ the results of Dalton and Wood are identical with ours.

Stephenson and Wood[40] have studied the classical isotropic Heisenberg ferromagnet in a uniform field and derived the free-energy series, F, to seventh order in the inverse temperature, K, and to tenth order in the field, h. The isothermal susceptibility series may be obtained from the free energy using the relation $\chi^b=-(\partial^2 F/\partial h^2)_K$. For $\tau=\Delta=0$ the resulting series agrees with ours through orders $k=6$ and $n_h=6$.

Pirnie *et al.*[41] have calculated the susceptibility series to sixth order for the isotropic Heisenberg model with nearest- and next-nearest-neighbor interactions. The series is given for arbitrary spin quantum number and ratio of the coupling constants J_2/J_1. In the limit $S=\infty$ and $h=0$ this series reduces to ours.

D. Analysis of the susceptibility series

In this section we present an analysis of the reduced staggered susceptibility series in Tables I and II. The functions $\bar{\chi}^s_{xx}$ and $\bar{\chi}^s_{zz}$ are expected to be divergent along the SF↔P and AF↔P boundaries, respectively. The series are analyzed for various values of $\tau=J_2/J_1$, Δ, and h.

In all cases investigated the ordering susceptibility is analyzed in terms of a simple power-law divergence

$$\bar{\chi}^s_{\alpha\alpha}(K)\sim(K_c-K)^{-\gamma},\quad \alpha=x,z\ , \tag{4.7}$$

where γ is the critical point exponent. Firstly, we have constructed Padé approximants, $[N,D]$, to the logarithmic derivative of the series

$$\frac{d}{dK}\ln\bar{\chi}^s_{\alpha\alpha}(K)\simeq[N,D]\sim\frac{\gamma}{K_c-K}\ . \tag{4.8}$$

$[N,D]$ denotes the ratio of two polynomials in K of order N and D, respectively. Using the pole distribution displayed by the Padé tables we have chosen appropriate Euler transformations

$$K^*(p)=\frac{K}{1+pK} \tag{4.9}$$

to improve the convergence of the series extrapolation procedures. p is a transformation parameter. In conjunction with the Padé analysis we have performed a ratio analysis with the Neville improvement to the Euler transformed series. We consider the series extrapolation procedure as having converged if the Padé and the Neville estimates of the critical temperature agree within 1–2%. In general, it turns out that the series in Tables I and II contain too little information to allow a reliable determination of the exponent γ.

We commence with the case of nearest-neighbor interactions alone; i.e., $\tau=0$. In this case the loose-packed sc lattice causes the ordering susceptibility to have a ferromagnetic singularity at $K_{c1}\sim -K_c$ in zero field. This situation is only slightly affected by the presence of the nonordering field. The ferromagnetic singularity interferes with the physical antiferromagnetic singularity, and consequently we have performed an Euler transformation with parameter $p\sim -K_{c1}^{-1}$. For $h=0$ the convergence of the series extrapolation is good for all values of Δ and gives results for the critical temperature which are consistent with the Monte Carlo calculations.[17] For $\Delta=0$ the system enters the spin-flop phase for an arbitrary finite value of the field h. Increasing the field we find for all values of Δ an increasing uncertainty in the series extrapolation procedures. In the isotropic case, $\Delta=0$, it is only possible to locate the phase boundary for $h\lesssim 3$. In this field regime the results are the same as Landau and Binder's results within a few percent. However, the series estimate of T_c is independent of the field within the uncertainty. In the case $\Delta=0.2$, which has also been investigated by Landau and Binder, the AF↔P phase boundary may be determined from the series for $h\lesssim 3$ and the result agrees with the Monte Carlo results within 5%. For $\Delta\neq 0$ we have not been able to locate the SF↔P boundary as the Padé tables contain only complex principal poles. These complex poles are situated close to the imaginary axis in the complex K plane, and for increasing fields the poles move rapidly towards the origin. The same characteristics of the pole distribution as a function of h are found for $\bar{\chi}^s_{zz}$ for $h\gtrsim 5$. We conclude that the sixth-order series for the ordering susceptibilities with $\tau=0$ contain insufficient information to allow a determination of the phase boundaries for fields $h\gtrsim 3$. This may be due to the fact that the large nonordering fields, which are needed to significantly affect the antiferromagnetic order, effectively decouple the pair interactions in the finite clusters of spins contributing to the low-order coefficients in the series expansion. This implies that the series contain a decreasing amount of

TABLE III. Estimates of the critical temperature as a function of the field $h=\mu H/J$ for transitions from the antiferromagnetic (AF) phase to the paramagnetic (P) phase and from the spin-flop (SF) phase to the paramagnetic phase. T_c^P is obtained from the diagonal elements $[N, 5-N]$ of the Padé table for the logarithmic derivative of the ordering susceptibility series, Eqs. (4.4) and (4.5). T_c^N denotes the estimate obtained from a Neville analysis. The series have been subjected to an Euler transformation. The ratio of next-nearest- and nearest-neighbor coupling constants is $\tau=-\frac{1}{2}$. The anisotropy parameter is $\Delta=0.05$. Temperatures are in units of J/k_B.

	AF ⟷ P transition T_c^P					SF ⟷ P transition T_c^P				
h	[4,1]	[3,2]	[2,3]	[1,4]	T_c^N	[4,1]	[3,2]	[2,3]	[1,4]	T_c^N
0.00	6.72	6.73	6.72	6.74	6.72					
2.00	6.52	6.53	6.51	6.64	6.58					
4.00	6.37	6.37	6.37	6.40	6.36					
4.50	6.26	6.26	6.25	6.26	6.26	6.17	6.20	6.18	6.25	6.16
4.75	6.19	6.19	6.18	6.19	6.20	6.19	6.19	6.17	6.24	6.15
5.00	6.12	6.12	6.09	6.10	6.15	6.17	6.17	6.17	6.22	6.14
5.25	6.05	6.05	6.00	6.00	6.07	6.16	6.16	6.16	6.21	6.12
5.50	5.97	5.97	5.90	5.90	6.02	6.16	6.15	6.25	6.15	6.10
6.00	5.79	5.79	5.64	5.64	5.85	6.14	6.14	6.14	6.13	6.10
7.00						6.09	6.09	6.09	6.09	6.07
8.00						6.05	6.03	6.06	6.06	6.06
9.00						6.01	5.96	6.05	6.05	6.05

information on the cooperative nature of the system for increasing fields. A similar problem was encountered in the series analysis of the nearest-neighbor spin-$\frac{1}{2}$ Ising antiferromagnet in a nonordering magnetic field.[4] To overcome this problem we may either calculate additional terms in the series or strengthen the connectivity of the spin system by including more interacting neighbors. The latter possibility is straightforward in our approach.

In the following we report the results in the case $\tau=-\frac{1}{2}$. We have analyzed the ordering susceptibility series in the range $\Delta\in[0,1]$ in order to determine the phase diagram as a function of the anisotropy parameter. It turns out that the two series may now be extrapolated to yield the critical temperature for $h\lesssim 6-8$ in the regions where the corresponding ordered structure is stable. Beyond the region of thermodynamic stability and for $h\gtrsim 6-8$ the series extrapolation breaks down. The breakdown may be indicated by one or more of the following observations: (i) the Padé and the Neville estimates of the critical temperature disagree, (ii) the Padé tables exhibit poor convergence, and (iii) the Padé tables contain only complex principal poles.

Table III illustrates the convergence of the series extrapolation for $\Delta=0.05$. The table compares the diagonal elements of the Padé table, T_c^P, with the Neville estimate of the critical temperature, T_c^N. The series have been subjected to the optimal Euler transformation, which in this case involves parameters $p\in[0,6]$. The table shows the regions of convergence for the two series.

E. Phase diagram

In Fig. 2 we show the phase boundaries for $\Delta=0$, 0.2, 0.4, and 0.8 in the case $\tau=J_2/J_1=-\frac{1}{2}$. The figure includes only the boundary between the paramagnetic phase and the phase which is the stable one down to $h=0$ for the corresponding value of Δ. The critical temperature at $h=0$, the Néel temperature $T_N^{\rm HT}=T_c^{\rm HT}$ $(h=0)$, is given for various values of Δ in Table IV. The table also includes the Néel temperature, $T_N^{\rm MF}$, estimated from the mean-field theory. $T_N^{\rm MF}$ is independent of the anisotropy and given by

$$k_B T_N^{\rm MF}/J=\tfrac{2}{3}(n_1-\tau n_2)\ , \tag{4.10}$$

where $n_1=6$ and $n_2=12$ are the number of nearest- and next-nearest-interacting neighbors. It is seen that the mean-field theory seriously overestimates the Néel temperature and gives a wrong prediction of the dependence of T_N on the anisotropy.

In the isotropic case, $\Delta=0$, the spin-flop phase boundary shown in Fig. 2 has a weak field dependence for small fields, and we have found no bulge in the phase boundary above the bicritical point. Our result is consistent with the Monte Carlo work on the nearest-neighbor model for which no umbilicus was found. Furthermore, recent experimental results[21] for the isotropic antiferromagnet $RbMnF_3$ show a depression of the order $2\times10^{-3}\,T_N$ at the umbilicus. For the low-anisotropy antiferromagnet $KNiF_3$ the depression is of the order $7\times10^{-4}\,T_N$.[19] These

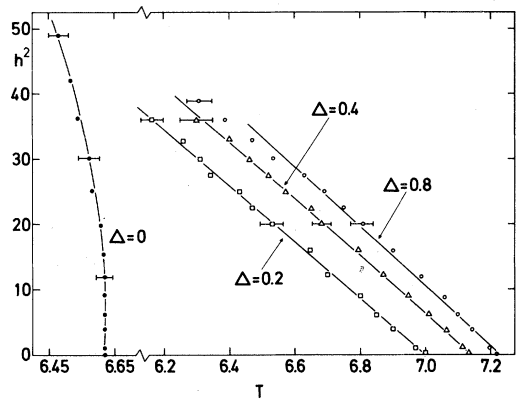

FIG. 2. (T,h) plane of the phase diagram for the anisotropic Heisenberg antiferromagnet in a uniform external field, $h=\mu H_{\|}/J$, along the easy axis. The phase boundary separating the antiferromagnetic phase and the paramagnetic phase is shown for $\Delta=0.2$, 0.4, and 0.8, where Δ is the anisotropy parameter. For $\Delta=0$ the figure shows the boundary separating the spin-flop phase and the paramagnetic phase. The various boundaries are estimated from a combined Padé and Neville analysis of the ordering susceptibility series, Eqs. (4.4) and (4.5). The error bars indicate typical confidence limits from the series analysis. The ratio of next-nearest- and nearest-neighbor coupling constants is $\tau=-\frac{1}{2}$.

depressions are below the resolution of the series calculations.

In the anisotropic cases, $\Delta\neq 0$, shown in Fig. 2 the phase boundaries AF$\leftrightarrow$P, are quadratic in the critical field for small fields:

$$h_c^2=A\,[T_N-T_c(h_c)]\ . \tag{4.11}$$

The quadratic relation Eq. (4.11) is consistent with the mean-field prediction for $h<h_b$, where h_b is the bicritical field.[36] For $\Delta=0.2$ and 0.4 the relation is valid for all values of the field for which the series may be analyzed. For $\Delta\gtrsim 0.6$ there is an increasing deviation with increasing Δ at high fields. It appears from Fig. 2 that the constant A in Eq. (4.11) is independent of the anisotropy for $\Delta\neq 0$.

We have not been able to locate the phase boundary separating the spin-flop phase and the paramagnetic phase for the anisotropic cases shown in Fig. 2. The reason for this may be clarified by a simple mean-field calculation. According to the mean-field theory the bicritical field is given by

$$\mu h_b^{\mathrm{MF}}/J=(n_1-\tau n_2)[\Delta(2-\Delta)]^{1/2}\ . \tag{4.12}$$

For the least anisotropic case shown in Fig. 2, $\Delta=0.2$, the bicritical field is $h_b^{\mathrm{MF}}(\Delta=0.2)=7.20J/\mu$ which is at the boundary of the field region in which the series can reliably be extrapolated.

We have therefore carried out the series analysis for $\Delta=0.05$ and $\Delta=0.10$. In both cases the SF$\leftrightarrow$P transition line can be located. The resulting phase diagrams are shown in Fig. 3. The two second-order phase boundaries have been calculated beyond stability in order to determine the *bicritical point*, (T_b,h_b). In the case $\Delta=0.10$ the bicritical point appears at the boundary of the field region in which the series for $\bar{\chi}_{zz}^{s}$ may be extrapolated. Similar to the isotropic case in Fig. 2 there is no indication of a bulge in the SF$\leftrightarrow$P phase boundary above T_b. We expect that our finite series are too short to expose the bicritical point as an umbilicus.

The values of the bicritical temperature and the bicritical field determined from the analysis are given in Table IV. The corresponding values obtained from the mean-field theory are included for comparison. According to the mean-field theory the bicritical temperature, T_b^{MF}, to first order in $(T_N^{\mathrm{MF}}-T_b^{\mathrm{MF}})/T_N^{\mathrm{MF}}$ is

TABLE IV. Néel temperatures $T_N=T_c(h=0)$, bicritical temperatures T_b, and bicritical fields $h_b=\mu H_b/J$, estimated from mean-field theory (MF) and from high-temperature series analysis (HT) of the ordering susceptibility. Temperatures are in units of J/k_B. Δ is the anisotropy parameter. The ratio of next-nearest- and nearest-neighbor coupling constants is $\tau=-\frac{1}{2}$.

Δ	T_N^{MF}	T_N^{HT}	T_b^{MF}	T_b^{HT}	h_b^{MF}	h_b^{HT}
0.00	8.00	6.60±0.02				
0.05	8.00	6.71±0.01	7.40	6.14±0.05	3.75	4.9±0.3
0.10	8.00	6.84±0.01	6.80	5.70±0.07	5.23	6.6±0.5
0.20	8.00	7.00±0.01				
0.40	8.00	7.13±0.01				
0.60	8.00	7.19±0.01				
0.80	8.00	7.22±0.01				
1.00	8.00	7.24±0.01				

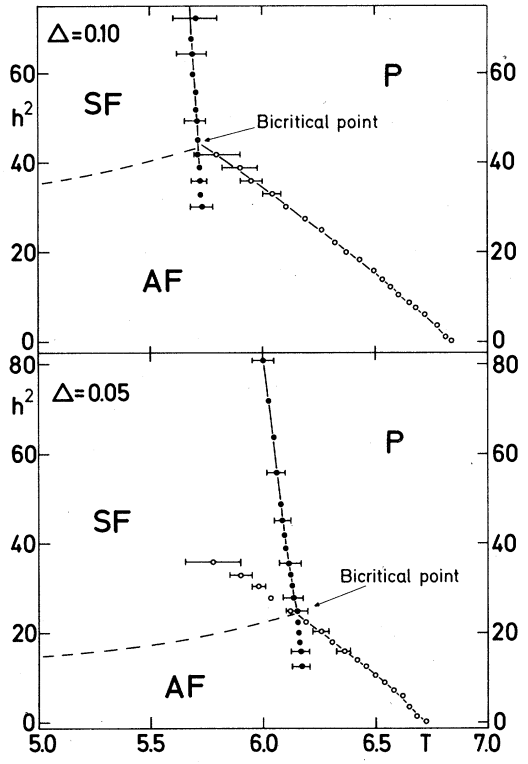

FIG. 3. (T,h) plane of the phase diagram for the anisotropic Heisenberg antiferromagnet in a uniform external field, $h=\mu H_{\|}/J$, along the easy axis. The phase diagram is shown in the two cases $\Delta=0.05$ and 0.10, where Δ is the anisotropy parameter. The figure shows the boundaries separating the spin-flop phase (SF), the antiferromagnetic phase (AF), and the paramagnetic phase (P) (cf. Fig. 1). ● indicates points obtained from a series analysis of $\bar{\chi}^{s}_{xx}$, and ○ indicates points obtained from a series analysis of $\bar{\chi}^{s}_{zz}$, Eqs. (4.4) and (4.5). The solid lines are drawn as a guide to the eye. The dashed lines indicating the SF ↔ AF transitions are drawn qualitatively. The error bars indicate typical confidence limits from the series analysis. The ratio of next-nearest- and nearest-neighbor coupling constants is $\tau=-\frac{1}{2}$.

given by[36]

$$T_b^{\mathrm{MF}} \simeq T_N^{\mathrm{MF}}(1-\tfrac{3}{2}\Delta) \ . \tag{4.13}$$

Table IV shows that the mean-field theory overestimates the bicritical temperature. However, the ratios,

$$T_b^{\mathrm{MF}}(\Delta=0.05)/T_N^{\mathrm{MF}}(\Delta=0.05)=0.93$$

and

$$T_b^{\mathrm{MF}}(\Delta=0.10)/T_N^{\mathrm{MF}}(\Delta=0.10)=0.85 \ ,$$

are close to the corresponding values 0.92 and 0.83, respectively, predicted from the series analysis. These considerations show that the mean-field theory reliably predicts the position of the bicritical point relative to the Néel point. Furthermore, the mean-field theory underestimates the bicritical fields h_b but the ratios $h_b^{\mathrm{HT}}/h_b^{\mathrm{MF}}$ are the same for $\Delta=0.05$ and 0.10.

It should be noted that for our model the actual locations of the critical and bicritical points have previously been predicted solely by the mean-field theory. The renormalization-group calculations[12–14] provide only estimates of universal critical parameters (e.g., critical exponents) and the functional form of the phase boundary close to the bicritical point. Our series estimate of T_b as well as the position of the boundaries in the vicinity of the bicritical point is too inaccurate to determine the appropriate linear scaling fields.[42] Therefore, we cannot probe the renormalization-group predictions of the form of the phase boundaries and the value of the crossover exponent.[14]

F. Conclusions of Sec. IV

In this section we have derived high-temperature series expansions of various susceptibilities for the classical anisotropic Heisenberg antiferromagnet in a nonordering magnetic field along the anisotropy axis. The series are analyzed to provide the phase diagram spanned by the temperature and the field. The general correlation function series presented in Ref. 32 may be used to determine further aspects of the complete phase diagram by including various other ordering or nonordering fields.

The ordering susceptibility series to sixth order for the nearest-neighbor model contain insufficient information to locate the various phase boundaries. By inclusion of next-nearest neighbors with stabilizing ferromagnetic interactions the series may be extrapolated for fields $\mu H/J \lesssim 6-8$. The resulting phase diagram, which qualitatively describes antiferromagnetic materials such as $CuCl_2\cdot 2H_2O$, $GdAlO_3$, $MnCl_2\cdot 4H_2O$, FeF_2, MnF_2, $RbMnF_3$, and $KNiF_3$, is consistent with the predictions of renormalization-group calculations and Monte Carlo simulations. The position of the various phase boundaries and the bicritical point are calculated as functions of the anisotropy. The results demonstrate that the mean-field theory is inadequate in a quantitative description of the phase diagram, but qualitative predictions such as the quadratic field dependence of the phase boundary close to the Néel point are consistent with the series results. The results in this section show that field-dependent critical phenomena of complicated systems may to a large extent be investigated by high-temperature series analysis.

V. DISCUSSION

The method described in this paper is capable of treating general Hamiltonians. The practical limitations of the method are set by the capacity of the computer utilized. The calculations described in this article were performed on a Cyber 173 and required computing times of the order of several days. We believe that the fastest current computers may add an extra term to our sixth-order series in roughly the same computing time, but the general nature of our approach makes it insuperably difficult to get any further. We suggest that further progress should be obtained by teaching the computer how to recognize general symmetries of the interaction graphs appearing in step (i) of Sec. II.

Because our series extend only to sixth order, it is impossible to determine critical parameters with the high accuracy which characterizes series analyses based on model-specific expansion techniques. However, the large number of model parameters, which we can include in the series coefficients, makes it possible to determine phase diagrams and critical behavior of antiferromagnetic model systems for which series analysis has not previously been practicable. The series results presented in Sec. IV for the phase diagram of the anisotropic Heisenberg antiferromagnet in a field demonstrate that our approach is indeed useful.

It is our hope that this work and especially the general expressions for the correlation functions series[32] may stimulate use of high-temperature series analysis of models for various spin systems subjected to magnetic fields.

---

[1]See for example *Phase Transitions and Critical Phenomena,* edited by C. Domb and M. S. Green (Academic, New York, 1974), Vol. 3.

[2]Details of the method as well as applications to various antiferromagnetic models are described in O. G. Mouritsen, Ph.D. thesis (University of Aarhus, 1979) (unpublished).

[3]For a description of the moment method in high-temperature series work and its relation to other current methods, see for example G. S. Rushbrooke, G. A. Baker, Jr., and P. J. Wood in Ref. 1, p. 245.

[4]A. Bienenstock, J. Appl. Phys. 37, 1459 (1966); A. Bienenstock and J. Lewis, Phys. Rev. 160, 393 (1967).

[5]D. C. Rapaport and C. Domb, J. Phys. C 4, 2684 (1971).

[6]F. Harbus and H. E. Stanley, Phys. Rev. B 8, 1141, 1156 (1973); M. Wortis, F. Harbus, and H. E. Stanley, *ibid.* 11, 2689 (1975).

[7]M. Plischke and D. Zobin, Can. J. Phys. 55, 1126 (1977).

[8]M. Ferer, Phys. Rev. B 18, 6265 (1978).

[9]S. J. Knak Jensen, O. G. Mouritsen, E. Kjaersgaard Hansen, and P. Bak, Phys. Rev. B 19, 5886 (1979).

[10]O. G. Mouritsen and S. J. Knak Jensen, Phys. Rev. B 18, 465 (1978).

[11]P. Pfeuty, D. Jasnow, and M. E. Fisher, Phys. Rev. B 10, 2088 (1974).

[12]D. R. Nelson, J. M. Kosterlitz, and M. E. Fisher, Phys. Rev. Lett. 33, 813 (1974).

[13]M. E. Fisher and D. R. Nelson, Phys. Rev. Lett. 32, 1350 (1974).

[14]J. M. Kosterlitz, D. R. Nelson, and M. E. Fisher, Phys. Rev. B 13, 412 (1976).

[15]P. R. Gerber and M. E. Fisher, Phys. Rev. B 13, 5042 (1976).

[16]M. Kerszberg and D. Mukamel, Phys. Rev. B 18, 6283 (1978).

[17]D. P. Landau and K. Binder, Phys. Rev. B 17, 2328 (1978).

[18]L. J. de Jongh and A. R. Miedema, Adv. Phys. 23, 1 (1974).

[19]C. C. Becerra, Y. Shapira, and N. F. Oliveira, Jr., Phys. Rev. B 18, 5060 (1978).

[20]A. R. King and N. Rohrer, Phys. Rev. B 19, 5864 (1979).

[21]Y. Shapira and C. C. Becerra, Phys. Rev. Lett. 38, 358, 733(E) (1977); Y. Shapira and N. F. Oliveira, Jr., J. Appl. Phys. 49, 1374 (1978); Phys. Rev. B 17, 4432 (1978).

[22]J. A. J. Basten, E. Frikkee, and W. J. M. de Jonge, Phys. Rev. Lett. 42, 897 (1979).

[23]C. Domb, in *Phase Transitions and Critical Phenomena,* edited by C. Domb and M. S. Green (Academic, New York, 1974), Vol. 3, p. 1.

[24]C. Domb and M. F. Sykes, Philos. Mag. 2, 733 (1957).

[25]M. F. Sykes, J. W. Essam, B. R. Heap, and B. J. Hiley, J. Math. Phys. 7, 1557 (1966).

[26]S. J. Knak Jensen and E. Kjaersgaard Hansen, Phys. Rev. B 7, 2910 (1973).

[27]E. Ambler, J. C. Eisenstein, and J. F. Shooley, J. Math. Phys. 3, 118 (1962).

[28]M. Wortis, in *Phase Transitions and Critical Phenomena,* edited by C. Domb and M. S. Green (Academic, New York, 1974), Vol. 3, p. 113.

[29]J. L. Martin, in *Phase Transitions and Critical Phenomena,* edited by C. Domb and M. S. Green (Academic, New York, 1974), Vol. 3, p. 97.

[30]M. E. Fisher and B. J. Hiley, J. Chem. Phys. 34, 1253 (1961).

[31]D. D. Betts, in *Phase Transitions and Critical Phenomena,* edited by C. Domb and M. S. Green (Academic, New York, 1974), Vol. 3, p. 569.

[32]See AIP document No. PAPS PLRBA-22-3256-11 for 11 pages of general correlation function series. Order by PAPS number and journal reference from American Institute of Physics, Physics Auxiliary Publication Service, 335 East 45th Street, New York, N.Y. 10017. The price is $1.50 for each microfiche (98 pages), or $5 for photocopies of up to 30 pages with $0.15 for each additional page over 30 pages. Airmail additional. Make checks payable to the American Institute of Physics. This material also appears in *Current Physics Microform,* the monthly microfilm edition of the complete set of journals published by AIP, on the frames immediately following this journal article.

[33]R. B. Griffiths, Phys. Rev. Lett. 24, 715 (1970); Phys. Rev. B 7, 545 (1973).
[34]C. J. Gorter and T. van Peski-Tinbergen, Physica (Utrecht) 22, 273 (1956).
[35]H. Rohrer and H. Thomas, J. Appl. Phys. 40, 1025 (1969).
[36]K. W. Blazey, H. Rohrer, and R. Webster, Phys. Rev. B 4, 2287 (1971).
[37]D. Mukamel, Phys. Rev. B 14, 1303 (1976).
[38]A. D. Bruce and A. Aharony, Phys. Rev. B 11, 478 (1975).
[39]D. W. Wood and N. W. Dalton, J. Phys. C 5, 1675 (1972). See also J. G. Brankov and B. S. Sidjimov, *ibid.* 11, L209 (1978).
[40]R. L. Stephenson and P. J. Wood, Phys. Rev. 173, 475 (1968).
[41]K. Pirnie, P. J. Wood, and J. Eve, Mol. Phys. 11, 551 (1966).
[42]M. E. Fisher, Phys. Rev. Lett. 34, 1634 (1975).